

Recent advances in fuel cell technology at Ballard

Jürgen Stumper*, Charles Stone

Ballard Power Systems, 9000 Glenlyon Parkway, Burnaby, BC V5J 5J8, Canada

Available online 2 September 2007

Abstract

This paper presents an overview of some of the key challenges and issues that need to be overcome in the area of performance and durability to achieve commercial-viable PEM fuel cell technology¹. While there has been significant progress towards these objectives in the last few years, fundamental understanding of the factors resulting in performance loss and materials degradation is still lacking. Several key elements in overcoming these challenges, such as in situ diagnostic tools, modelling and simulation and accelerated stress tests are discussed. A general framework for the improvement of performance degradation and durability is presented in order to achieve the US DOE cost target of USD 30 kW_{net}⁻¹ for the fuel cell stack, while advancing operational imperatives such as freeze start, higher temperature operation and reduced reliance on external humidification. © 2007 Elsevier B.V. All rights reserved.

Keywords: Fuel cells; Diagnostic tools; Water management; Durability; Accelerated testing; Modelling

1. Introduction

Over the last several years there have been significant improvements in proton exchange membrane fuel cell (PEMFC) technology, which mainly have been capitalized in increased performance and durability while reducing cost per kilowatt of power produced. In most cases these improvements have been driven by fundamental understanding related to unit cell component failures, design optimization and sophisticated operating strategies. For example, membrane degradation driven by free radical attack related to species produced during side-reactions of the fuel cell is now also well understood. Based on this understanding, several approaches have been developed by suppliers leading to improved materials chemistry, by the use of additives to intercept the damaging free radicals and by control of operating conditions to minimize the conditions that accelerate the rate of degradation. Durability impacts are also seen in structural changes and collapse of anode and cathode electrocatalyst layers and the mitigation of failures related to reactant gas starvation, stop/start operation, poor water management and freeze start are well established in many new fuel cell systems. This has been achieved by the development of new catalysts, improved catalyst support materials, optimized electrocatalyst layer struc-

tures, enhanced flow field design and significant improvements in fuel cell stack and system controls. Not often discussed, but nevertheless a critical unit cell material and stack design element is the sealing technology used to ensure that unit cell gas shorting, plate-to-plate electrical shorting and containment of reactant gases are controlled. Ballard has developed significant tools, modelling and simulation capabilities to fine-tune the required design elements of fuel cell stack sealing and, in working with key suppliers, has optimized the materials, while advancing related unit cell design elements to mitigate chemical and mechanical failures of sealing materials. Ballard has also developed and employs sophisticated and validated CFD and FEA modelling to ensure that reactant gas manifold design and related unit cell gas distribution is managed to minimize issues like current density fluctuations and uncontrolled “hot spots” within the fuel cell stack. Many in situ tools have also been developed and employed to identify spatial current density and temperature distribution, as well as membrane and electrocatalyst layer resistance as a function of effective water management. Even more sophisticated tools and testing methodologies have been developed to accelerate known failures and thereby help in the effective and efficient evaluation of new materials, designs and operating strategies. These tools, models and related fundamental understanding have resulted in significant improvements in performance and durability. These are two of the key characteristics essential to the achievement of Ballard’s technology “Road Map”. In March of 2005, Ballard published its technology “Road Map”, outlining the required improvements in cost

* Corresponding author.

E-mail address: jurgen.stumper@ballard.com (J. Stumper).

¹ http://www.ballard.com/be_informed/fuel_cell_technology/roadmap.

reduction, durability, volumetric power density and freeze start capability required to meet commercial targets for the stack subsystem of a fuel cell vehicle. These objectives are in many cases strongly aligned with the US Department of Energy (US DOE) targets, determined to define the level of capability required to achieve commercial viability for the fuel cell stack for automotive applications. Achievement of these goals will require continued strategic component supplier collaborations, funding of specific academic research projects and continued collaboration with original equipment manufacturers. In this regard, Ballard is fortunate to have both substantial and significant collaborations with unit cell component suppliers as well as joint research efforts and field trials, with DaimlerChrysler, Ford and Ebara Corporation, including working closely with system integrators like general hydrogen and Cellex. In addition, Ballard co-funds of numerous academic research projects to enhance fundamental understanding, modelling and simulation expertise, and the development of breakthrough materials for the future. Advances in fundamental understanding, tools development, modelling and simulation, as substantial means of advancing PEMFC durability, are described in detail in the following sections.

2. In situ diagnostic tools for the analysis fuel cell performance

2.1. Analysis of cell voltage losses

The breakdown of the observed cell voltage losses into activation, ohmic and mass transport related losses, the so called voltage loss breakdown (VLB) is of fundamental importance to the improvement of cell performance and reduction of performance degradation. Whereas there are direct measurement methods available for the ohmic loss of a fuel cell, only indirect methods have been reported in the literature for the determination of activation and mass transport loss. For example, as the plot of a purely activation limited polarization curve yields a straight line in an E_{cell} versus $\log(j)$ representation, the mass transport loss can be determined from the non-linearity of an IR-corrected E_{cell} versus $\log(j)$ curve as the difference between the straight line extrapolation from low current densities ($<0.1 \text{ A cm}^{-2}$) and the IR-corrected E_{cell} versus $\log(j)$ curve. Using this procedure the overall VLB can be determined if the ohmic cell resistance is known from other methods. There are several methods published in the literature that allow the direct determination of the ohmic cell resistance under in situ conditions such as (a) AC impedance spectroscopy [1], (b) AC impedance at 1 kHz [2], (c) the current interrupt method [3], (d) H_2/O_2 polarization at high stoichiometries [4] and (e) the MRED method [5].

Due to the consumption of reactants along the flow channels the local operating conditions such as reactant pressure, temperature, relative humidity, etc. are in general not constant over the active area, particularly under real-life operation. This has important implications for both cell performance and performance degradation as they are dependent on the local operating conditions and consequently also show spatial variation. To dis-

tinguish between different failure modes it is therefore necessary to understand the interrelation between structural and physico-chemical properties, operating conditions and performance on a local level, which requires the capability to determine the VLB with spatial resolution over the active area. This is possible using an extension of the methods mentioned before such as (a) AC impedance spectroscopy [6] and (b) the MRED method [7]. Through a combination of the MRED method with current mapping it is possible to obtain further information on the local distribution of kinetic, ohmic and mass transport losses across the cell area. For example, profiles of the membrane resistance along the flow channel can be obtained, which provide important information about localized membrane drying.

In addition, dynamic phenomena such as transient drying and re-hydration of the membrane can be investigated by monitoring changes in current distribution over time [7]. Such investigations are particularly interesting for automotive applications, which are characterized by fast dynamic load cycles with high turn-down ratios leading to non-stationary operation over significant time periods. Through the investigation of changes in the ohmic resistance over time, the water distribution in the cell under such non-stationary conditions can be studied, the control of which is of crucial importance for the improvement of fuel cell performance and durability.

2.2. Distribution of ohmic voltage losses across components of the unit cell

In addition to spatial resolution within the active area (x - y) it is also important to attribute the voltage loss types to the different cell components (VLB-C) such as flow field plate, gas diffusion layer (GDL), catalyst layer and membrane, thereby gaining spatial resolution also in the through-plane, (z) direction. As an example, in the case of voltage degradation due to increased mass transport loss it is important to know how much of this mass transport loss increase is caused by O_2 diffusion through the GDL and the catalyst layer, respectively. There are very few papers available that address the VLB-C experimentally but Büchi [8] have used thin gold wires as probes within the membrane in combination with the current interrupt method to measure its ohmic resistance with spatial resolution in the x - y plane, whereas Watanabe et al. [9] utilized Pt-wires.

We have recently shown that it is possible to determine the contributions of fuel cell components such as flow field plate, GDL and membrane to the total ohmic loss of the fuel cell by insertion of Pt micro-wires into the fuel cell (see Fig. 1). The experiments were performed with $25 \mu\text{m}$ Pt-wires (Goodfellow) that were inserted into the MEA of a small area test cell before bonding (wires 2 and 3) and during cell assembly (wires 1 and 4). Wires 2 and 3 were chosen with $5 \mu\text{m}$ polyester insulation, which was removed in a 5–10 mm long section located in the middle of the MEA, whereas wires 1 and 4 were bare Pt. All wires were in electrical contact with both adjacent fuel cell components.

Fig. 2 shows the experimental results for a polarization curve measured on an MEA with four Pt micro-wires arranged as in Fig. 1 and demonstrates that such an arrangement can be used to

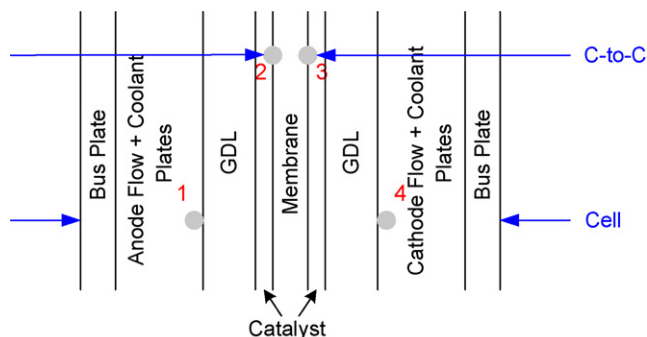


Fig. 1. Schematic arrangement of the Pt μ -wires within the unit cell. Wires were numbered sequentially from 1 to 4: wire 1: between anode flow field plate and GDL; wire 2: between anode catalyst and membrane; wire 3: between cathode catalyst and membrane; wire 4: between cathode flow field plate and GDL. Cell voltages and catalyst-to-catalyst voltages were measured between the bus plates and wires 2 and 3, respectively.

measure the voltage distribution through the unit cell. The voltages for the two polarization curves were measured between the two bus plates and anode/cathode catalyst layer, respectively. As expected the catalyst-to-catalyst voltage is higher than the bus plate voltage and the voltage difference increases linearly with current. This confirms that the voltage losses between catalyst layer and bus plate are essentially ohmic in nature. Fig. 2 also shows a more detailed breakdown of the ohmic loss into the different cell components giving the individual contributions of gas diffusion electrode (GDE) and flow field plate to the total the ohmic cell resistance. The results show that the voltage losses in the flow field plates together account for 70% of the non-membrane ohmic losses, which provides important direction for further improvements in cell performance. The contribution of the ohmic resistance of the membrane to the cell resistance can be determined using AC-impedance spectroscopy on wires 2 and 3 or from a mass transport free catalyst-to-catalyst polarization curve obtained using the MRED method [5]. The validity of the latter approach has been shown through the observed linear dependence of membrane ohmic resistance upon membrane thickness.

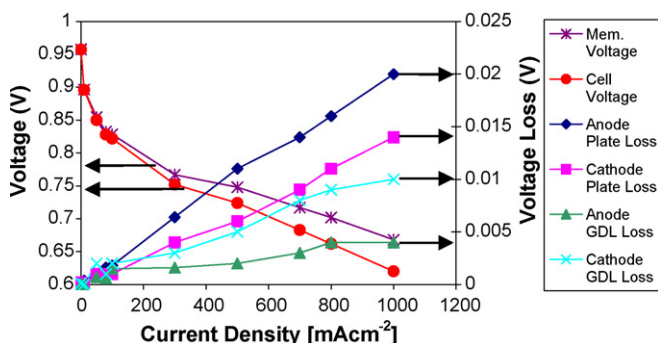


Fig. 2. Polarization curves measured in a small area test cell between bus plates and wires 2 and 3 (catalyst-to-catalyst) together with voltage differences between anode bus plate and wire 1 (anode plate loss, diamonds), cathode bus plate and wire 4 (cathode plate loss, squares), wires 1 and 2 (anode GDL loss, triangles) and wires 3 and 4 (cathode GDL loss, crosses).

3. Water distribution within the unit cell

Liquid water plays a key role in PEM fuel cells because its presence is closely linked to the functionality and durability of the main components of the unit cell. For example, the ionic conductivity of the most commonly used perfluorosulfonic acid (PFSA) electrolyte membrane Nafion[®] increases almost linearly with water content. Therefore, the water content of the membrane should be larger than a threshold value (minimum condition) under all operating conditions. Furthermore, the durability of PFSA membranes is also strongly impacted by water, insufficient hydration can lead to mechanical stress in the membrane that promotes failures such as tearing and cracking [10]. It also has been shown that low relative humidity operation accelerates chemical degradation of proton exchange membranes [11,12]. Membrane degradation can be further accelerated by relative humidity cycling compared to steady-state operation [13]. The GDE can be divided into the GDL and the catalyst layer (CL). The CL mainly consists of catalyst particles, ionomer and pore space each of which are critical for the formation of the interface where the electrochemical reactions take place. If the CL contains too little water, its ionic conductivity will drop and not all of the catalyst surface will be accessible, which will contribute to resistive and kinetic cell voltage losses. Further, reduced reactant gas solubility in the ionomer will cause increased mass transport losses. Too much liquid water on the other hand will impede reactant gas transport in the void space and lead to mass transport related performance losses. Consequently, the water content of the catalyst layer should lie between a minimum and a maximum value (optimum condition). Similar to the membrane, water management plays an important role also for the degradation of the catalyst because both Pt dissolution–precipitation and corrosion of the carbon support are accelerated by increased reactant gas humidity [14].

In contrast, the GDL water content should be less than a maximum value (maximum condition) as liquid water in the GDL will impede gas transport from the flow channels to the catalyst layer. Similarly, the amount of liquid water in the channels should also obey a maximum condition as the presence of liquid water in the flow channels increases gas flow resistance, which in turn increases the parasitic load of supplying the reactant gases and may cause flow sharing issues between adjacent cells in a stack or fuel channels within a cell.

Because water management is critical for durability and performance of PEM fuel cells, Ballard has been developing advanced diagnostic tools to study the distribution and movement of water within the unit cell. Among the requirements for such diagnostic tools are (i) in situ applicability, (ii) minimal invasiveness and (iii) ability to provide local information, i.e., information on the distribution of liquid water over the active area. To date, there is only one diagnostic method known to the authors that fulfills all three of the above requirements: neutron-imaging. However, the necessary neutron sources are available only at few research institutes worldwide equipped to deal with radioactive radiation. Another method that fulfills requirements (i) and (iii) is magnetic resonance imaging. A key feature of this method is the capability to determine the liquid water dis-

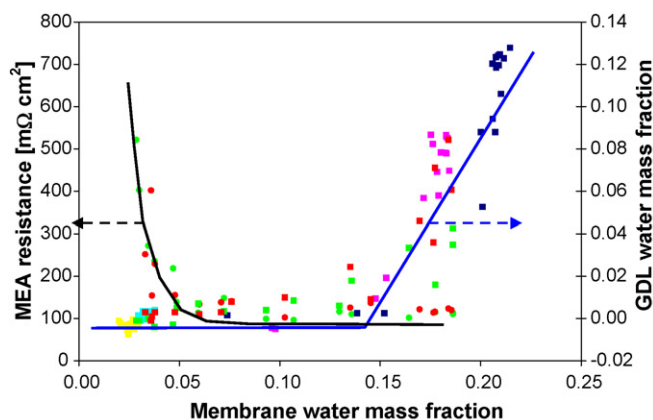


Fig. 3. Water distribution in the MEA as function of membrane water content. GDL water mass fraction comprises mass fraction for both anode and cathode GDL combined. Symbols: experimental values; lines: guide to the eye.

tribution through the membrane [15], although the size of the fuel cells that can be investigated is limited due to mechanical restrictions.

Fig. 3 shows the typical results for water management within an MEA under operation. The MEA resistance was determined in situ using the MRED method whereas the membrane and GDL water mass fractions were determined gravimetrically after physical separation of the GDL from the membrane. It can be seen that there is a narrow band of optimum membrane water content between 5% and 15% water content outside of which either the membrane resistance dramatically increases or the GDL starts to flood. Membrane drying is known to decrease MEA durability whereas both membrane drying and GDL flooding reduce fuel cell performance [16].

In addition to the distribution of water within the MEA, the distribution of liquid water droplets in the flow channels is of great importance for reliable fuel cell stack operation, especially under low-stoichiometry conditions or during start-up. The presence of liquid water in one of several parallel flow channels leads to an increase in flow resistance which reduces the gas flow and in turn leads to increased liquid water formation thus setting up a feedback loop that can lead to a non-even flow distribution across the channels. Moreover, the flow distribution may exhibit multiple steady states [17].

The distribution of liquid water in a fuel cell under operation has been studied by a number of authors both by using *n*-imaging [18] as well as direct visualization [19,20]. This latter method has also been used at Ballard on a full size (300 cm² active area) fuel cell. Current mapping was also integrated as described in Ref. [7] allowing the correlation between local current density and liquid water content.

An optical setup using a fast digital camera in combination with automated image processing allowed the quantitative determination of the total liquid water content as well as the distribution over the active area under quasi steady-state conditions. Using this tool, the water distribution in the cathode flow field was investigated over a wide range of operating conditions. Fig. 4 shows a typical result for the distribution of liquid water droplets across the active area of the cell. Proceeding from left to right in

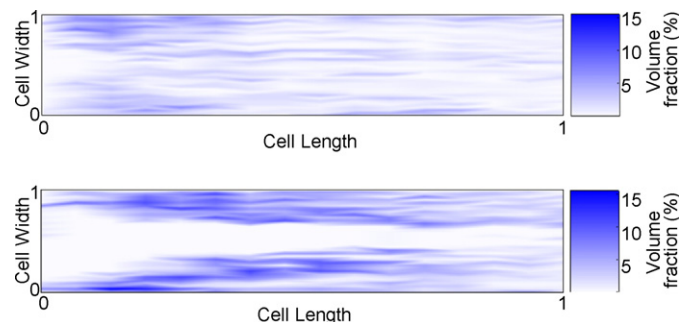


Fig. 4. Two-dimensional water maps of stationary water droplets in the cathode flow channels obtained experimentally with a full size fuel cell modified for flow visualization (aspect ratio adjusted for clarity). Reactant inlets: left; outlets: right. Operating conditions: co-flow operation; current density: 1.0 A cm⁻²; anode RH: 100%. (a): cathode RH: 100% and (b) cathode RH: 50%.

the direction of the reactant gas flow, three distinct regions can be distinguished: at the inlet and outlet, respectively, which show lower water content and a middle region showing an elevated number of stationary water droplets. A possible explanation for this could be the existence of a dry region at the inlet in particular for RH < 100% preventing the formation of liquid water in the channels, whereas at the outlet the increased liquid water flux in the channels leads to frequent clearing of the channels through travelling water slugs preventing droplet formation. More interestingly, a distinct “wedge”-shaped pattern is observed in the direction perpendicular to the channels. When plotted against the cell width, the water content shows a minimum at the channels in the middle of the cell indicating a similar behaviour for the flow resistance across the channels. While the setup does not allow for a direct measurement of the gas flow velocity in the channels, it is plausible to assume that most of the reactant gas flows through the middle channels. These results illustrate the role that flow visualization can play for the optimization of flow distribution within a fuel cell under two-phase flow conditions as well as for the validation of model calculations.

Another important aspect related to water management is water crossover between anode and cathode. The combination of water production and water crossover determines the total water amount that needs to be removed through the flow channels. If the localized water crossover is known, then the total water flux distribution can be calculated using the measured current distribution in order to understand the observed liquid water distributions. To this end, Ballard has developed a novel experimental method to measure water crossover and water crossover distributions [21,22].

Water crossover between anode and cathode side is sometimes expressed through the water transfer factor α by forming the ratio of crossover flux and product water formation. The water transfer factor is determined by three different mechanisms: electro-osmotic drag, diffusion and convection. The water transfer factor has been found to be a determining aspect in the membrane's hydration state and hence its conductivity although it has seldom been reported in the literature. This can be explained by the difficulty in achieving water balance measurements that are accurate enough to allow for an accurate determination of the water flux across the membrane. The water

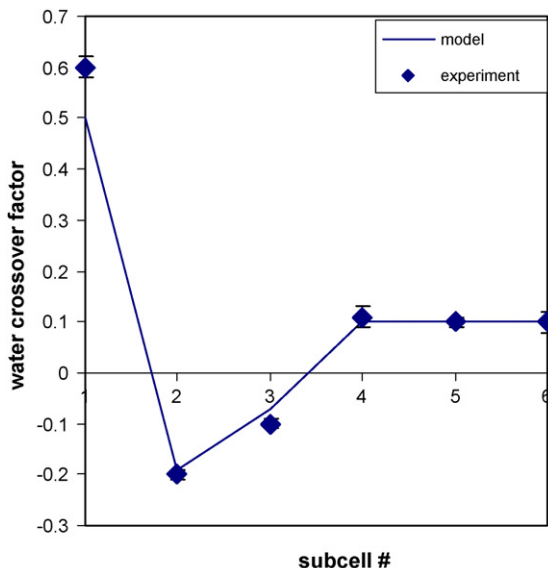


Fig. 5. Profile of the water crossover factor α from anode to cathode along the length of the flow channels. Symbols: experimental results; line: model calculations. Operating conditions: H_2/air , co-flow; current density: 0.27 A cm^{-2} ; anode/cathode stoich: 1.6/1.8; anode/cathode dew point: $63/38^\circ\text{C}$; $T_{\text{in}} = 65^\circ\text{C}$; $T_{\text{out}} = 69^\circ\text{C}$.

balance measurements are complicated further by the two-phase nature of the flows exiting the PEMFC's. Janssen [23] and Voss et al. [16], have generated data that allows for the calculation of the overall water transfer factor in PEMFC stacks by water collection on the PEMFC stack outlet streams whereas Mench et al. [24] reported in situ water concentration measurements. They used a gas chromatograph to measure amongst other things the water content of the gas-phase. Despite the limited experimental data available for the water transfer factor on PEMFC's, several efforts focusing on the individual contributing mechanisms have been published in the past two decades. It's chiefly through the results from such efforts that model studies [25–27] were able to predict the water transfer factor for PEMFC's. The setup employed in our experiments uses IR-absorption sensors in combination with complete evaporation of any liquid water enabling highly accurate water crossover determination independent of the amount of liquid water present [21].

Fig. 5 shows the results of a water transfer factor distribution obtained using a sub-cell approach. Experimentally, the 300 cm^2 were divided into six consecutive 50 cm^2 sub-cells and one water crossover experiment was devoted to each of the sub-cells. The individual sub-cells were run at a current density that was predicted using model calculations averaged over the sub-cell area. The first sub-cell saw the same conditions as the full size cell and the following sub-cell was fed inlet conditions based on the load current and measured water transfer factor for the previous sub-cell. This process was repeated sequentially from inlet to outlet until all the sub-cells were measured. The figure shows a strong dependence of water transfer factor along the flow channel length, exhibiting a strong water crossover from the anode to the cathode in the inlet region due to the comparatively dry cathode (inlet RH = 38%). At the sec-

ond sub-cell the direction of water crossover reverses due to the quick humidification of the cathode gas and then reverses again back to the anode–cathode direction stabilizing around $\alpha = 0.1$ for the last three sub-cells, most likely due to the continued hydrogen consumption leading to saturation of the anode stream. These results show that advanced in situ tools can provide important insights on water management in PEM fuel cells which is characterized by a complex interaction of phenomena such as two-phase flow in channels, multiple steady states in channel networks and the coupling between fluid flows and electrical current within the active area and in proton exchange membranes.

4. Modelling and simulation

To reduce development cost and product development cycle times there is a strong need for modelling and simulation tools that can be used to evaluate different design alternatives with respect to performance and durability. Such models are necessary to gain predictive capability regarding the various structural and physicochemical properties of the fuel cell components and how they impact performance as defined by the customer requirements. The main challenge for fuel cell models is the number and complexity of the contributing phenomena, such as for example coupled heat-, mass- and charge-transport, two-phase flow, phase changes (vapour–liquid–ice) and interfacial electrochemical reaction kinetics which have to be accurately represented in 3D. This challenge can be addressed in two ways: (a) through a systematic framework similar to computational fluid dynamics (CFD) [27] or (b) through simplified first principles models focusing on a specific issue that limit the number of processes and/or reduce dimensionality to 1D or 2D. Ballard has utilized both approaches; using CFD calculations for mass transport to optimize flow distribution while minimizing pressure drop for channels in a flow field plate and cells in a stack (see Fig. 6) and through the development of several first principle models.

Recently, we developed a simplified model for water management in a polymer electrolyte membrane fuel cell [28]. The consumption of gases in the flow field channels, coupled to the electric potential and water content in the polymer membrane, was modeled in a two-dimensional slice from inlet to outlet and through the membrane. Both co- and counter-flowing air and fuel streams were considered and current density distributions were calculated as function of inlet humidity, gas stream composition and fuel and oxygen stoichiometry. The parameter describing the non-equilibrium kinetics of the membrane/catalyst interface was found to be fundamental to accurate fuel cell modelling and a new parameter which models non-equilibrium membrane water uptake rates was introduced. Overall, four parameters, the exchange current, a membrane water transfer coefficient, an effective oxygen diffusivity and an average membrane resistance, are fit to a subset of data and used for predictions of polarization curves, current density and membrane hydration distributions, water transfer and stoichiometric sensitivity. The comparison between model results and experimental data suggested that a majority of current production occurs at catalyst

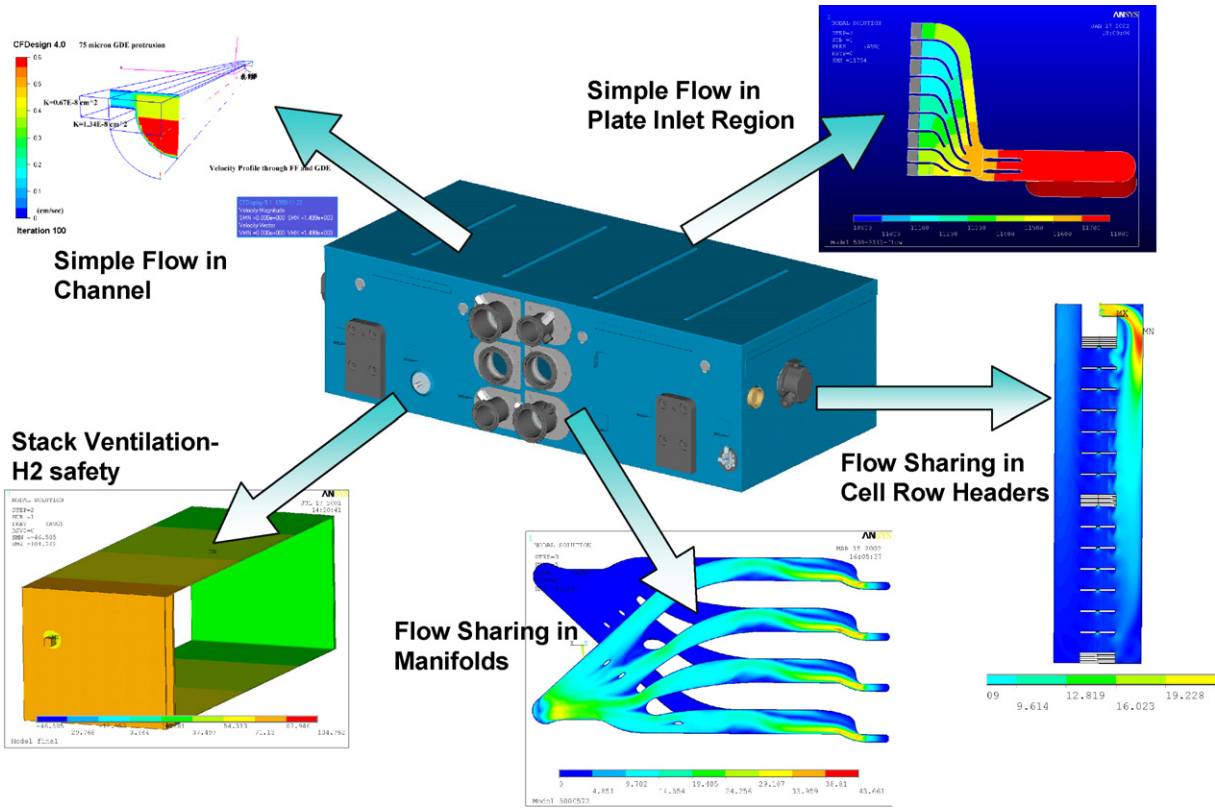


Fig. 6. Schematic representation for the application of CFD modelling: single phase flow in channels, flow field plate inlet, cell row header, stack manifold and stack enclosure ventilation.

sites within the membrane and that oxygen diffusion through membrane water plays a significant role in mass transportation losses. The value for the effective oxygen diffusivity from channel to catalyst derived from experiments was roughly one order of magnitude below the free space value. Further experiments revealed that O_2 diffusion is limited not by the GDL, but the catalyst layer [5].

Some important performance aspects such as, for example, cell voltage variability and low cell voltages are only observable in fuel cell stacks and Ballard has made significant progress in the understanding of how fuel cell component properties can influence cell voltage distribution. For example, an electrical stack model was developed that can explain the characteristic signatures observed during cell voltage scans along the number of cells in a stack. For example, the characteristic “V” signature of the cell voltages often observed around a low cell can be explained as a consequence of the redistribution of the electrical current in the stack “around” a low performing section of the active area in the anomalous cell. It was further shown that the number of neighbouring cells affected increases with decreasing bipolar plate conductivity [29]. This electrical interaction stack model has recently been complemented by a stack flow distribution and performance model that also includes the coupling between electrical current distribution and reactant consumption along the flow field channels. Fig. 7 shows how manufacturing variability can affect the cell voltage scan along a stack [30]. The figure also reproduces the exper-

imentally observed phenomenon that the so-called “low cells” are often observed towards one end of the stack. Furthermore, the calculations showed that the cell-to-cell voltage variability depends critically on oxidant stoichiometry. This illustrates how such models can be very useful in the design process for the development of tolerance requirements, which are an essential element to meet the cost, functional quality and durability targets.

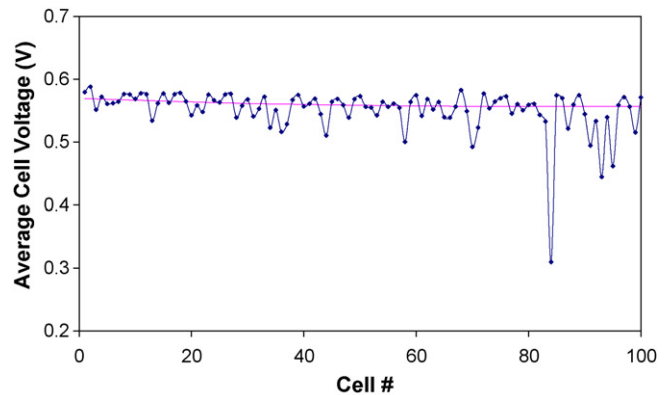


Fig. 7. Average cell voltage distribution vs. cell # in a 100-cell stack calculated for a random variability of the cathode channel friction factor (S.D. 20%) around the design value. Operating conditions: U-type manifold (reactant gas in/outlets at cell 0), counter-flow; H_2 /air pressure: 320/284 kPa; H_2 /air stoichiometry: 1.2/1.8; current density: 1.25 A cm^{-2} .

5. Performance degradation/durability improvements through optimization of cell design and operating conditions

To achieve commercially viable fuel cell technology for automotive applications, the following must be improved: cost reduction, improved volumetric power density, fuel cell performance and increased durability to 5000 h. In addition, depending on the hybridization strategy, these targets need to be achieved under fast dynamic operation and dramatically reduced external humidification over a wide temperature range, including sub-zero start-up. To meet these requirements the following capabilities, amongst others, need to be further improved:

- Understanding of the relationships between cell structure, physicochemical properties, operating conditions and performance.
- Mechanistic understanding of performance degradation.
- The development of accelerated test methods to reduce design iteration/evaluation times.

There exists no comprehensive review discussing cell structure–performance relationships for PEM fuel cells, however, the impact of some of MEA structural aspects on beginning-of-life (BOL) cell performance are discussed in Gasteiger et al. [2] and Kocha [31]. Flow field plates are discussed by Wilkinson et al. [32] including the use of flow field design to optimize reactant distribution and water management. In regards to water transport within the porous electrode structure, however, major knowledge gaps still exist regarding the multi-phase (liquid–vapour) behaviour of water in porous electrode structures. The capillary pressure and its dependence on liquid water content inside the electrode, which is a key driver for liquid water transport [33], is currently unknown and model calculations have to rely on functions derived from soil or sand. Consequently, collaborations with academic institutions to develop more realistic descriptions of the capillary pressure and its dependence on liquid water saturation are required.

Mechanistic understanding of fuel cell performance degradation comprises (a) the identification of the responsible unit cell component (s) and quantification of their relative contribution to performance degradation, (b) the quantification of component structural and/or physicochemical property changes over time and (c) detailed understanding of the processes leading to these structural/property changes. An overview of available experimental methods to address (a) and (b) has been published by Wilkinson et al. [4] whereas a detailed understanding of many causes and degradation mechanisms is still lacking. Among the operational factors known to impact performance degradation are reactant gas impurities, operating conditions such as temperature, RH, reactant stoichiometry and steady state *versus* dynamic operation. Among the structural changes known to occur are catalyst particle size growth [34], transfer leak formation [35] and crystallinity change [36] in the proton

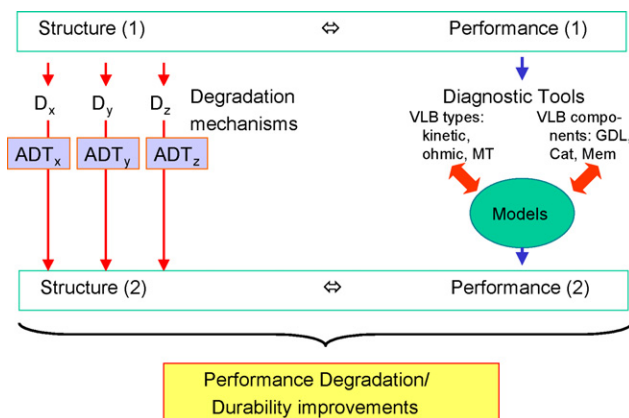


Fig. 8. Schematic diagram illustrating the approach for improvement of performance and durability. ADT: accelerated durability test; MT: mass transport; Cat: catalyst; Mem: membrane.

exchange membrane. Overall, the available literature on degradation mechanisms has focused mainly on the membrane [37] and catalyst. As an example, both particle agglomeration as well as dissolution/re-precipitation has been proposed as mechanisms for Pt particle size growth [38].

Fig. 8 illustrates in a schematic diagram how the application of the aforementioned in situ diagnostic tools (VLB, VLB-C) during accelerated life testing in combination with state-of-the-art ex situ characterization methods can help to provide deeper insights into how structural changes caused by a particular degradation mechanism affect fuel cell performance. Advanced in situ diagnostic tools allow the identification of the responsible fuel cell component(s) which can then be characterized with state-of-the-art ex situ characterization methods to determine the nature of the structural changes and identify causes for performance degradation. The structural characterization results also provide important inputs for the validation of degradation models that can be used to identify critical degradation parameters and to set design requirements. Fig. 9 shows an example, where the effect

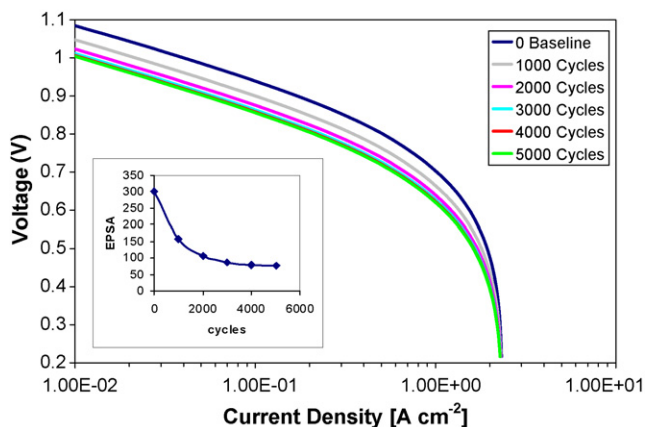


Fig. 9. Calculated effect of a loss in cathode catalyst activity during voltage cycling (see inset) on the polarization curve for a PEM fuel cell. EPsA denotes the product of the active Pt surface area $A_{Pt,MEA}$ ($m^2 g^{-1}$) and the cathode Pt loading ($mg cm^{-2}$).

of a decrease in electrochemically active Pt surface area of the cathode catalyst on cell voltage has been calculated assuming a first order kinetics for the dependence of ECA(t) [39] and a one-dimensional model of a complete MEA [40]. Such model calculations are useful for example to translate the allowable cell voltage degradation into requirements for catalyst stability, which are expected to become more stringent as Pt loading is reduced.

Finally, the study of the influence of operational stress factors as well as cell design and materials selection on performance degradation becomes a valuable avenue to (a) gain insight into the mechanism(s) that lead to structural changes, (b) develop accelerated durability tests (ADT) and (c) identification of mitigation strategies. Mechanistic understanding requires understanding the role of all promoting/inhibiting parameters and operating conditions as well as their respective limits outside of which different mechanisms might come into play. The resulting fundamental understanding allows the development of accelerated tests that are essential to reduce design iteration/evaluation times and develop mitigation strategies.

6. Conclusion

This paper presents recent advances in fundamental understanding, tools development, modelling and simulation at Ballard and their role in progress the objectives of its automotive technology “Road Map” targets for cost reduction, durability, volumetric power density and freeze start capability. It is shown how advanced tools for performance diagnostics, ex situ structural characterization and accelerated durability tests form key elements of an overall strategy for the improvement of performance and durability.

The detailed information provided through the breakdown of cell voltage loss into the different types and the attribution of cell voltage losses to the different fuel cell components in combination with ADT tests and structural characterization provides a powerful framework for (a) the identification of degradation mechanisms and (b) the development of mitigation strategies for performance degradation to improve durability and performance. Furthermore, the development and improvement of models for the dependence of performance on structure and operating conditions enables the prediction not only of performance but also performance degradation by incorporating the observed changes in structure/operating conditions *versus* time. This approach enables the identification of the key relationships between performance and durability on one hand, and key component characteristics and operating conditions on the other, critical to advancing fundamental understanding that will accelerate materials development and design improvement, leading to commercial-viable fuel cell technology in the shortest, most cost-effective manner.

Acknowledgements

The authors wish to thank M. Tam, A. Roshanzamir, S. Hamada and P. Sauriol for the conduction of experiments, D.

Harvey, P. Sauriol and P. Chang for model calculations and J. Kenna for preparation of Fig. 6.

References

- [1] B. Andreaus, A.J. McEvoy, G.G. Scherer, *Electrochim. Acta* 47 (2002) 2223.
- [2] H.A. Gasteiger, W. Gu, R. Makharia, M.F. Mathias, B. Sompalli, in: W. Vielstich, A. Lamm, H.A. Gasteiger (Eds.), *Handbook of Fuel Cells*, vol. 3, Wiley, Chichester, 2003, p. 593.
- [3] M.V. Williams, H.R. Kunz, J.M. Fenton, *J. Electrochem. Soc.* 152 (2005) A635.
- [4] D.P. Wilkinson, J. St-Pierre, in: W. Vielstich, A. Lamm, H.A. Gasteiger (Eds.), *Handbook of Fuel Cells*, vol. 3, Wiley, Chichester, 2003, p. 611.
- [5] J. Stumper, H. Haas, A. Granados, *J. Electrochem. Soc.* 152 (2005) A837.
- [6] I.A. Schneider, *J. Electrochem. Soc.* 152 (2005) A2092.
- [7] J. Stumper, M. Loehr, S. Hamada, *J. Power Sources* 143 (2005) 150.
- [8] F.N. Büchi, G.G. Scherer, *Proceedings of the second International Symposium on Proton Conducting Membrane Fuel Cells*, Boston, Massachusetts, 1998, p. 71.
- [9] M. Watanabe, H. Igarashi, H. Uchida, F. Hirasawa, *J. Electroanal. Chem.* 399 (1995) 239.
- [10] V. Stanic, M. Hoberecht, *Fuel Cell Seminar Abstracts*, 2004, p. 85.
- [11] T.D. Jarvi, E. Teather, *Fuel Cell Seminar Abstracts*, 2004, p. 81.
- [12] E. Endoh, *Electrochem. Solid State Lett.* 7 (2004) A209.
- [13] S. Motupally, T. Jarvi, *Proceedings of the 208th Meeting of the Electrochemical Society*, Los Angeles, 2005, p. 1167 [Abstract].
- [14] D.A. Stephens, M.T. Hicks, G.M. Haugen, J.R. Dahn, *J. Electrochem. Soc.* 152 (2005) A2309.
- [15] S. Tsushima, K. Teranishi, K. Nishida, S. Hirai, *Magn. Reson. Imag.* 23 (2005) 255.
- [16] H.H. Voss, D.P. Wilkinson, P.G. Pickup, M.C. Johnson, V. Basura, *Electrochim. Acta* 40 (1995) 321.
- [17] M. Ozawa, K. Akagawa, T. Sakaguchi, *Int. J. Multiphase Flow* 15 (1989) 639.
- [18] R. Satija, D.L. Jacobson, M. Arif, S.A. Werner, *J. Power Sources* 129 (2004) 238.
- [19] K. Tüber, D. Pocza, C. Hebling, *J. Power Sources* 124 (2003) 403.
- [20] F.Y. Zhang, X.G. Yang, C.Y. Wang, *J. Electrochem. Soc.* 153 (2006) A225.
- [21] P. Sauriol, G.-S. Kim, X. Bi, J. Stumper, J. St-Pierre, *AICHE Annual Meeting*, Cincinnati, OH, USA, 2005, p. Ref # 215b.
- [22] P. Sauriol, X. Bi, J. Stumper, D.S. Nobes, D. Kiel, *Proceedings of the first Int. Symp. on Fuel Cell and Hydrogen Technologies*, Calgary, AB, Canada, Canadian Inst. of Mining, Metallurgy and Petroleum, Montreal, Quebec, 2005, p. 531.
- [23] G.J.M. Janssen, *J. Power Sources* 101 (2001) 117.
- [24] M.M. Mench, Q.L. Dong, C.Y. Wang, *J. Power Sources* 124 (2003) 90.
- [25] T.E. Springer, T.A. Zawodzinski, S. Gottesfeld, *J. Electrochem. Soc.* 138 (1991) 2334.
- [26] A.Z. Weber, J. Newman, *Chem. Rev.* 104 (2004) 2334.
- [27] C.Y. Wang, *Chem. Rev.* 104 (2004) 4727.
- [28] P. Berg, K. Promislow, J. St-Pierre, J. Stumper, B. Wetton, *J. Electrochem. Soc.* 151 (2004) A341.
- [29] G.-S. Kim, J. St-Pierre, K. Promislow, B. Wetton, *J. Power Sources* 152 (2005) 210.
- [30] P.A. Chang, J. St-Pierre, J. Stumper, B. Wetton, *J. Power Sources* 162 (2006) 340.
- [31] S.S. Kocha, in: W. Vielstich, A. Lamm, H.A. Gasteiger (Eds.), *Handbook of Fuel Cells*, vol. 3, Wiley, Chichester, 2003, p. 538.
- [32] D.P. Wilkinson, O. Vanderleeden, in: W. Vielstich, A. Lamm, H.A. Gasteiger (Eds.), *Handbook of Fuel Cells*, vol. 3, Wiley, Chichester, 2003, p. 313.
- [33] U. Pasaogullari, C.Y. Wang, *J. Electrochem. Soc.* 151 (2004) A399.
- [34] J. Xie, D.L. Wood, K.L. More, P. Atanassov, R.L. Borup, *J. Electrochem. Soc.* 152 (2005) A1011.

- [35] J. Yu, T. Matsuura, Y. Yoshikawa, M.N. Islam, M. Hori, *Electrochem. Solid State Lett.* 8 (2005) A156.
- [36] C. Huang, K.S. Tan, J. Lin, K.L. Tan, *Chem. Phys. Lett.* 371 (2003) 80.
- [37] A.B. LaConti, M. Hamdan, R.C. MacDonald, in: W. Vielstich, A. Lamm, H.A. Gasteiger (Eds.), *Handbook of Fuel Cells*, vol. 3, Wiley, Chichester, 2003, p. 647.
- [38] P.J. Ferreira, G.J.I.O.Y. Shao-Horn, D. Morgan, R. Makharia, S. Kocha, H.A. Gasteiger, *J. Electrochem. Soc.* 152 (2005) A2256.
- [39] M.K. Debe, A.K. Schmoekkel, R.T. Atanasoski, G.D. Vernstrom, *J. Power Sources* 161 (2006) 1002.
- [40] A.A. Shah, G.-S. Kim, W. Gervais, A. Young, K. Promislow, J. Li, S. Ye, *J. Power Sources* 160 (2006) 1251.